THE MICROWAVE EMISSION SPECTRUM OF COLLIDING CHARGED WATER DROPS

by

Joe Keeney

Submitted to the Faculty of the
New Mexico Institute of Mining and Technology
in partial fulfillment of the requirements for the degree of

Doctor of Philosophy in Geoscience

June 1968

ABSTRACT

Water drops bearing different electric charges and colliding in air may emit electromagnetic energy on collision. Laboratory investigation of the microwave emission from 1.05 ± 0.02 millimeter diameter drops with equal and opposite charges reveals a spectral maximum in the neighborhood of 10,000 MHz (λ = 3 centimeters) and the presence of detectable energy at 22,400 MHz (λ = 1.34 centimeters). At frequencies near 10,000 MHz the emission intensity increases approximately as the fifteenth power of the charge.

An estimate based on the magnitude of the emission intensity indicates that emission of this type from terrestrial atmospheric clouds is not likely to be significant in comparison with thermal (black body) emission at these frequencies for drops smaller than 0.46 millimeter diameter. Emission from larger drops may be detectable if the drop collision rate is sufficiently high and if the drops are highly charged.

On the assumption that the Venusian atmosphere contains clouds of charged water drops and that these clouds are dense at microwave frequencies, a possible contribution of 60°K to the apparent temperature due to drop discharge may be inferred from the spectral distribution of radiated energy found in this study and the observed changes in the Venusian brightness temperature with microwave frequency. The computed temperature contribution of 60°K implies a collision rate of 1.8×10^{-7} collisions per drop per second between 0.94 millimeter diameter drops bearing maximum charge over the Venusian cross section. The necessary collision rate decreases with increasing diameter for drops bearing maximum (disruption) charge.

ACKNOWLEDGEMENT

In the course of a problem such as this one which extends over a considerable period of time the seeds of ideas are, I am certain, planted at more or less odd times. This has doubtless happened to me. So, in this sense, I am indebted to all those people with whom I have had the pleasure of association during my stay at New Mexico Tech.

I am especially indebted to Dr. Marx Brook who has closely supported this endeavor with the necessary equipment and certain valuable suggestions proposed at appropriate times, and without whose encouragement this problem could not have been done. Paul Krehbiel, in particular, produced a useful suggestion at a rather sticky moment, thereby salvaging a bad day, and Kelly Summers gave valuable suggestions concerning the writing process.

Thanks are due also to Dennis Williams who skillfully executed the drafting, and to my wife, Rae, who helped with the typing.

Financial assistance was provided by the Office of Naval Research under contract Nonr 815(03) and by the National Science Foundation under grant GA 488.

J.W.K.

TABLE OF CONTENTS

LIST OF FIGURES

INTRODUCTION

Certain natural processes are subject to investigation by radiometric means. Dicke et al. (1946) have shown that the antenna temperature of a microwave radiometer in equilibrium with its environment is a function of the thermodynamic temperature and the microwave absorption along the path defined by the antenna beam. These authors went on to apply the method to the measurement of the microwave absorption by atmospheric water vapor and oxygen.

Lhermitte (1965) extended the concept to the measurement of liquid water in atmospheric clouds for drop sizes small compared to the wavelength. Unfortunately, the validity of this technique in sensing the liquid water content of clouds has been placed in question by the observation that pairs of water drops bearing sufficient electric charges of opposite sign emit microwave energy on collision (Atkinson and Sartor, 1966). Any contribution from this source to the energy arriving at a radiometer antenna would manifest itself as an apparent increase in antenna temperature above the temperature due to thermal emission from matter in the antenna beam.

The same question applies to observations of the apparent temperature of Venus (Plummer and Strong, 1965), which exhibits a frequency dependence over the range of 3,000 MHz to 30,000 MHz as measured by microwave radiometry. Indeed, Tolbert and Straiton (1962) have suggested that the drop discharge phenomenon might account for these anomalous temperature measurements.

These considerations have led to the study reported here, which is an experimental investigation of the microwave emission resulting

from the collision and discharge of oppositely charged water drops in air.

Miller et al. (1965) have examined the optical portion of the drop discharge emission spectrum. They conclude that the light emission can be attributed to the dielectric breakdown of air, the medium in which the drops are immersed. In other words, a spark occurs.

The conditions necessary for the occurrence of a spark discharge are not clear. Atkinson and Sartor (1966) have reported the probability of spark occurrence as a function of drop diameter and charge for pairs of drops of equal diameters and equal and opposite charges. These authors indicate that there exists a charge level above which the probability of spark is greater than 80%, and a lower level below which the probability is less than 20%. Both levels increase with diameter. One is tempted to conclude immediately that the onset of sparking is determined by the inter-drop electric field. However, if this is true, then drop distortion must become significant at larger diameters. The curves given by Atkinson and Sartor show a linear relation between threshhold charge and diameter d instead of the expected d^2 charge dependence for spherical drops. This may be a manifestation of the increasing importance of inertial forces over viscosity and surface tension forces.

The question of spark onset is an intriguing one, but it is beyond the scope of this work, which examines some consequences of the spark when it does occur. We have verified qualitatively that, for a given drop size, there does appear to be a value of charge below which each collision does not result in detectable light or radio emission. Those cases reported in the following study are those of considerably higher

charge, for which a spark occurs at each collision.

The problem of electromagnetic emission from drops has been treated analytically by Atkinson and Paluch (1966) who established upper and lower bounds on the total radiated energy per discharge. They base their treatment on the observation that the discharge time is less than 10^{-9} seconds and that the radio emission at 10,000 MHz is predominantly dipolar, i.e., plane polarized with electric vector parallel to the axis of the spark. The maximum energy is taken as the electrostatic energy contained in the interdrop capacitance (Appendix B).

$$W = \frac{1}{2} \frac{Q^2}{C} \quad \text{joules.}$$

The lower bound is found by minimizing the classical expression for the energy radiated by an accelerating dipole.

$$E_{min} = \left(\frac{1}{6\pi\varepsilon_o c^3} \int_t \ddot{p}^2 dt \right)_{min} \quad \text{joules.}$$

Application of the calculus of variations yields the minimizing form of the function $\ddot{p}(t)$.

$$\ddot{p}(t) = A \frac{t}{\tau}, \qquad -\tau \leq t \leq \tau, \qquad A \text{ constant,}$$

$$\text{if } \dot{p}(-\tau) = \dot{p}(\tau) = 0.$$

The corresponding energy spectrum, obtained from the Fourier transform of $\ddot{p}(t)$ is

$$S(x) = \frac{9 \sin^2 \theta \, (\Delta p)^2}{16\pi^2 c^3 \varepsilon_o R^2 \tau^2} \cdot \frac{1 + x^2 - 2x \sin 2x - \cos 2x + x^2 \cos 2x}{x^4} \cdot \frac{\text{joules}}{\text{meter}^2 \text{ Hz}}$$

where $x = 2\pi f \tau$

2τ = duration of discharge

Δp = dipole moment destroyed by the collision

θ = angle between dipole axis and line of sight

R = distance to observer.

$S(x)$ is zero at the origin (zero frequency) and increases to a maximum at a frequency given by $f = 1/(3\tau)$ approximately. $S(x)$ yields the minimum radiated energy when integrated over all frequencies. However, it is only one of a large number of possible intensity functions, and there is no guarantee that it correctly describes the radiation intensity. In fact, the observed intensity does not fit this function.

The analytic treatment can be extended by showing that, in general, if $\dot{p}(-\tau) = \dot{p}(\tau) = 0$, then the spectral intensity function, whatever its form, must vanish at the origin. Define the duration of the discharge, 2τ, to extend over the interval $-\tau \leq t \leq \tau$. Assume $\dot{p}(-\tau) = \dot{p}(\tau) = 0$. We may define

$$\dot{p}(t) \equiv \int_{-\tau}^{t} \ddot{p} \, dt.$$

Then $\dot{p}(\tau) = \int_{-\tau}^{\tau} \ddot{p}\, dt = \dot{p}(\tau) - \dot{p}(-\tau) = 0.$

Also $\dot{p}(\tau) = \int_{-\tau}^{\tau} \ddot{p}\, dt = 2\tau \times (\text{average value of } \ddot{p}) = 0.$

Taking the Fourier transform of $\ddot{p}(t)$, provided $\ddot{p}(t)$ satisfies the Dirichlet conditions in every finite interval and $\int_{-\infty}^{\infty} |\ddot{p}|dt$ exists, we have

$$\ddot{P}(f) = \int_{-\tau}^{\tau} \ddot{p}(t)\, e^{-i2\pi ft}\, dt$$

and $\ddot{P}(0) = \int_{-\tau}^{\tau} \ddot{p}(t)\, dt \equiv 0$ Q.E.D.

The assumption appears to be a reasonable one, and so it is concluded, a priori, that the observed spectral intensity will probably vanish at the origin. We have also shown that the average value of $\ddot{p}(t)$ is zero.

The following paper is the result of an experimental investigation of the microwave emission intensity in the range of frequency between 7200 MHz and 22,400 MHz resulting from the collision of pairs of 1.05 millimeter diameter drops bearing equal and opposite charges. The emission intensity is defined as the energy per unit solid angle per unit frequency, with electric vector parallel to the line of discharge ($\cos \phi = 1$) and propagated in a direction perpendicular to the line of discharge ($\sin \theta = 1$).

EXPERIMENTAL METHOD

In this experiment the first requirement was a supply of charged water drops. The drop generator shown in Figures 1 and 2 performed this function in the manner described by Atkinson and Miller (1965). The process consisted of modulating the flow of water through a hypodermic needle with a small in-line pump. By careful coordination of needle size, flow rate, and pump drive frequency, the jet of water issuing from the needle could be caused to break up into a single stream of drops of uniform size and spacing (Figure 3).

Two continuous streams of drops were produced by the apparatus shown. The generator consisted of two movable carriages, each bearing a hypodermic needle and pump. The two carriages could be moved relative to each other with three degrees of freedom. The right-hand carriage was fitted with a worm drive providing motion transverse to the drop trajectory. The two drop streams were made to intersect with the adjustment. Horizontal spacing between the two carriages was controlled by another worm gear driving both carriages simultaneously. Finally, the angle of elevation of each drop stream was adjusted with a rotational worm drive on each carriage.

In operation the carriages were so adjusted that the two streams were coplanar, and at collision the line connecting the centers of colliding pairs was horizontal.

Electric charge was placed on each drop by induction (Figures 2 and 4). Each carriage was provided with a small wire ring mounted concentric with the drop stream and whose plane was perpendicular to the direction of drop motion. The rings were connected to high voltage

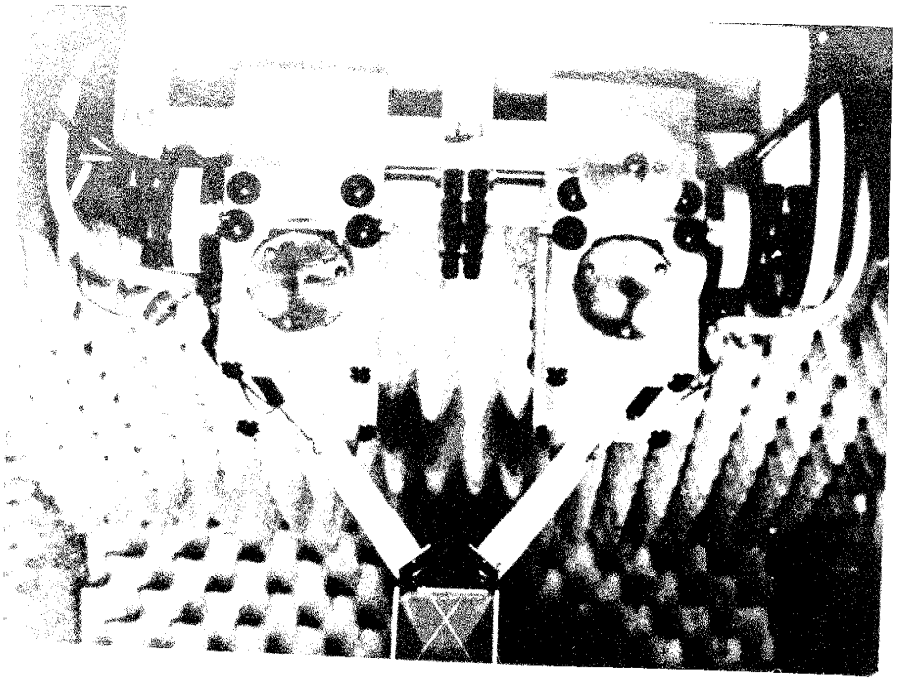

FIGURE 1. Drop generator, end view

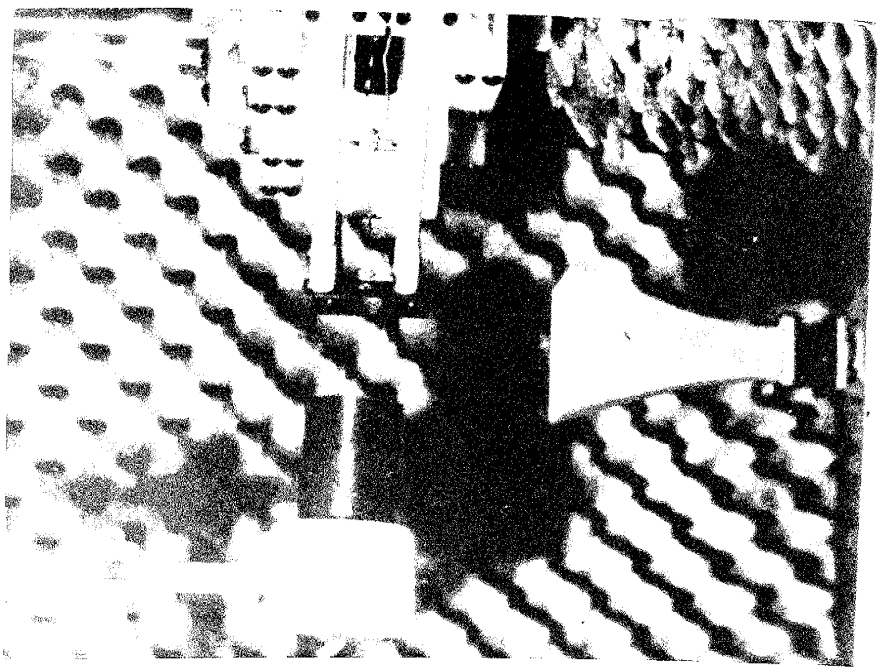

FIGURE 2. Drop generator, side view with charge measurement cup and microwave horn antenna

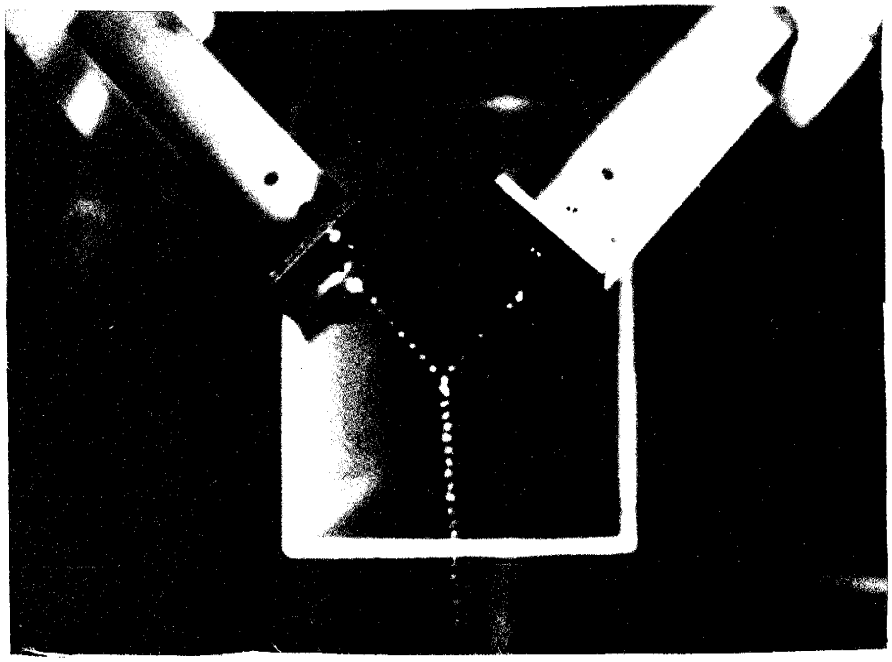

FIGURE 3. The geometry of drop encounters

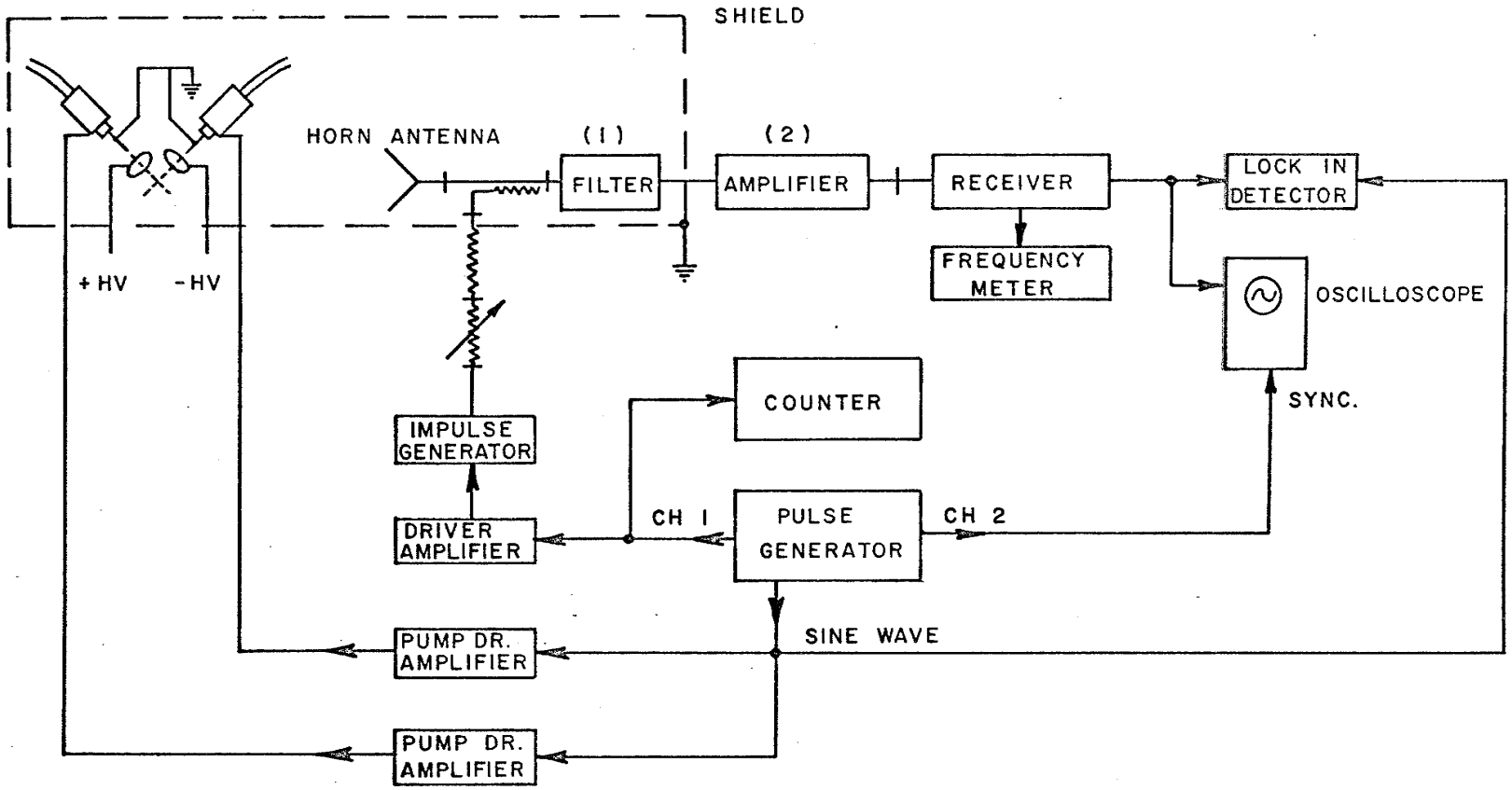

(1) Not available at 22.4 kmc.

(2) Not available at 10.4 and 22.4 kmc.

FIGURE 4. Basic configuration of experimental apparatus.

power supplies, one positive, the other negative. Each ring was mounted on a slide so that it could be placed near the point at which drops were formed. The rings were shielded with grounded brass plates mounted on the ends of the slides. This shielding effectively isolated the rings from each other and reduced the electric field in the region where drop collisions occurred. The charging circuit was completed by grounding the hypodermic needles.

The drop generator and the microwave detector were enclosed in a grounded metal box to provide isolation from external electric fields and air currents. The box was lined with microwave absorbing material to reduce reflections within the enclosure (Figures 5 and 6).

Figure 4 outlines the scheme employed to detect and measure the microwave energy emanating from colliding drop pairs. The sensing element was a standard gain microwave horn antenna so oriented that it sensed an electromagnetic wave whose electric vector was parallel to the line of drop centers, i.e., in the direction of the discharge. The range (the distance from discharge to horn aperture plane) was adjusted so that the discharge occurred in the far field (Fraunhofer region) of the antenna aperture.

$$R > \frac{D^2}{\lambda}$$

where D = width of aperture
and λ = wavelength.

Three different antennas were used to cover the range of frequency from 7200 MHz to 22,400 MHz. For the sake of convenience in reducing the observations the range was adjusted so that the antennas subtended

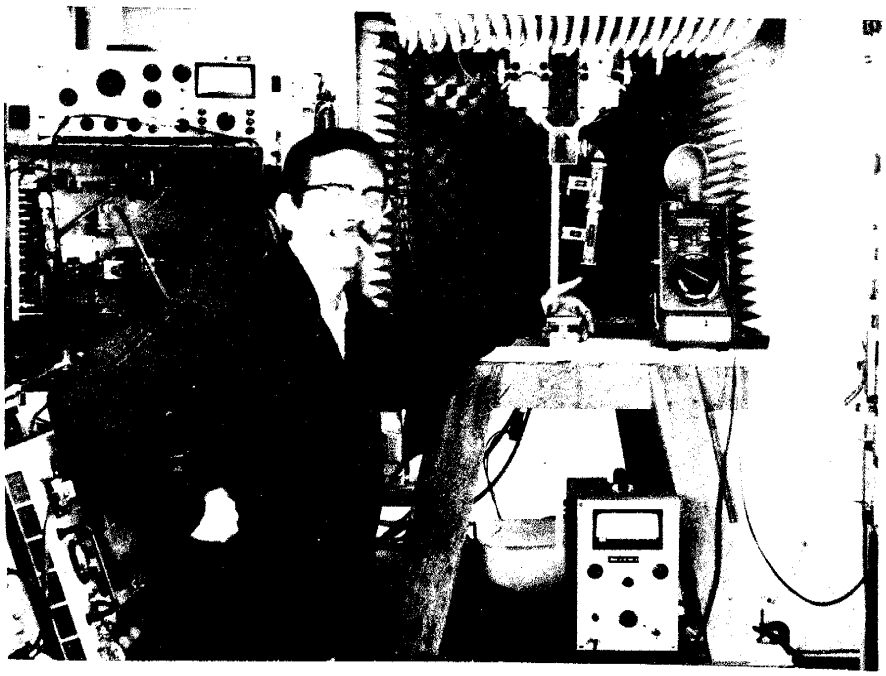

FIGURE 5. Observation chamber, end view with drop generator and microwave horn antenna in place

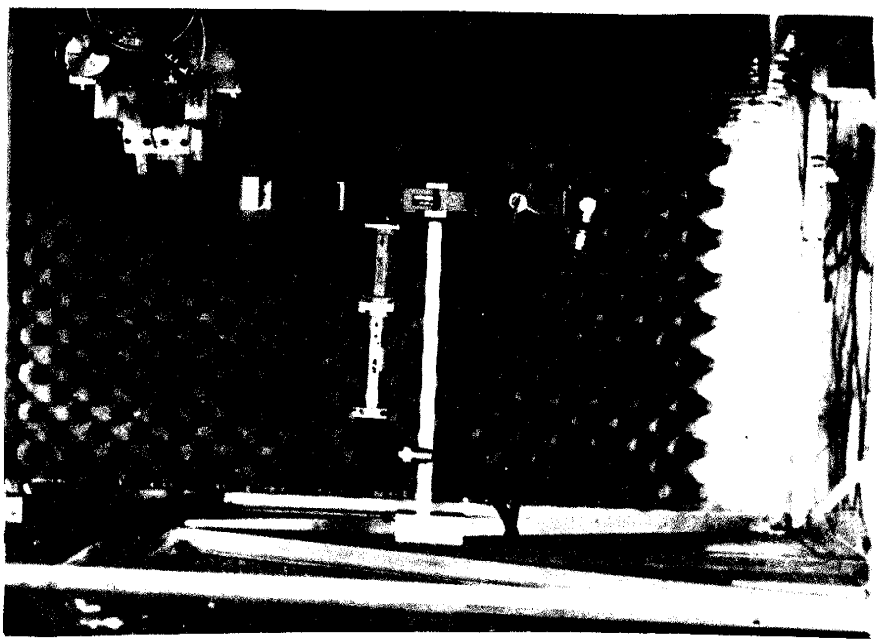

FIGURE 6. Observation chamber, side view with drop generator and microwave horn antenna in place

equal solid angles as seen from the discharge. Expressing the effective absorption cross section of the antenna as $G\lambda^2/4\pi$, where G is the gain, $G\lambda^2/4\pi R^2$ was made constant.

The measurement of energy so detected was accomplished by comparison with energy of known spectral intensity injected immediately after the antenna (Figure 4). The comparison standard was a Polarad Model 1C-120A Impulse Generator which produced very short pulses of uniform intensity between the frequencies of 1 MHz and 10,000 MHz. The instrument output is specified in terms of microvolts/MHz into a 50 ohm load. For present purposes, the datum energy level per pulse E_o was arbitrarily selected as that corresponding to 1 microvolt/MHz or 2×10^{-20} joules/MHz per pulse (Appendix A).

Two receivers were needed to cover the range of frequencies investigated.

The 7200 MHz intensity measurements were made with the Polarad Model R microwave receiver. This receiver is a triple frequency conversion superheterodyne type with an image rejection filter at the input. The sensitivity was rather low, so a low noise (7 db noise figure) high gain (30 db) travelling wave tube amplifier was employed to amplify the microwave signal ahead of the receiver (Figure 4). This arrangement increased the sensitivity sufficiently to permit the measurements reported here.

The NMIMT radiometer receiver had been built previously for atmospheric observations and it was used to make the present measurements at 9300, 10,400, and 22,400 MHz. It consisted of a balanced mixer with klystron local oscillator followed by an intermediate frequency

preamplifier and amplifier and a diode detector. The intermediate frequency was 60 MHz with bandwidth of 10 MHz. A bandpass amplifier at the detector output limited the effective bandwidth to about 1.5 MHz. At 9300 MHz two tunnel diode amplifiers with gain of 15 db each and noise figure of 5 db were available. These were placed in series in front of the mixer, increasing the sensitivity. Low noise preamplifiers were not available at the two higher frequencies.

A tunable bandpass filter with pass band of 10 MHz was employed at 9300 and 10,400 MHz. The filter accomplished image rejection and it acted to stretch the signal pulse before the pulse was mixed with the receiver local oscillator. The sensitivity of a superheterodyne receiver to signal pulses short with respect to a period of the local oscillator depends on the time (epoch) of reception with respect to the local oscillator (Atkinson and Abbott, 1967). That is, a short signal pulse arriving at the instant when the local oscillator signal goes through zero produces very little output, while a short pulse arriving at a local oscillator maximum produces maximum output. This is not thought to be a serious consideration in the present case because the comparison signal from the pulse generator is itself short--about 3.1×10^{-11} seconds as stated by the manufacturer. But the filter did tend to limit the signal bandwidth, a process which lengthened the pulses sufficiently to eliminate epoch sensitivity considerations. The filter also eliminated the image frequency band, improving the frequency resolution and signal to noise ratio.

Intensity measurements at 22,400 MHz were made without the aid of preamplifier or filter because these components were not available. A

certain amount of luck was involved here since the receiver was sensitive only to the strongest signal obtainable. Smaller signals were not detected.

A pulse generator drove the impulse generator and the drop generator so that one impulse was generated per signal pulse. A constant time relationship, adjustable by means of a time delay control built into the pulse generator, existed between each pair of pulses. The receiver output then consisted of a series of alternate signal and reference pulses. The receiver acted to select, amplify and detect the energy lying within a small range of frequency limited by the effective receiver bandwidth--about 1.5 MHz for both receivers used. Since the bandwidth was small, the spectral intensity of the signal, as well as that of the reference, may be regarded as uniform over the band of frequencies sampled. When viewed on the oscilloscope the drop discharge signal and the reference impulse signal were similar.

The signal level was ascertained simply by viewing the receiver output on the oscilloscope and adjusting the reference impulse level so that the amplitudes were equal. Changes in energy level of ± 1 db could be detected in this manner.

Alternatively, the signal and impulse levels were compared by applying the receiver output to the Lock-In Detector (Figure 4). The impulse was adjusted in time so that it occurred halfway between signal pulses. The two pulses were then compared in the detector with a sine wave of the same frequency (i.e., the pulse repetition rate) which in effect multiplied one pulse by +1, the other by -1, and added, a null output indicating equality of the two pulses.

Comparison on the oscilloscope was less complex and accomplished the same result, so the measurements at 7200, 9300, and 10,400 MHz were made in that way.

The energy measurement at 22,400 MHz was made by comparison with that at 10,400 MHz on the basis of receiver sensitivity.

Receiver sensitivities were determined by applying radio frequency pulses of 2 microsecond duration to the receiver at 10,400 MHz and 22,400 MHz and finding the power level at which the signal to noise ratio was unity. The sensitivity levels were found to be -89 dbm at 10,400 MHz and -92 dbm at 22,400 MHz as illustrated in Figure 7.

For charges of $\pm 105 \times 10^{-12}$ coulomb the signal at 10,400 MHz was just detectable with respect to noise. The fact that no signal was detected at 22,400 MHz for the same charges indicated that the energy was at least 3 db lower on account of the difference in receiver sensitivity at the two frequencies. The maximum level must be lower by another 3 db due to the signal treatment by the receiver. The receiver is heterodyne type, in which the incoming signal is mixed with a local oscillator and reduced in frequency in the mixer. There are two frequency bands (images) which may mix with the local oscillator, one above and one below the local oscillator frequency. The 10,400 MHz measurements were made with a waveguide filter which acted to select one or the other of these two bands, but no such filter was available at 22,400 MHz. Consequently, any detectable signal would represent twice the energy of a detectable signal with filter. Hence, the signal at 22,400 MHz must have been at least 6 db below that at 10,400 MHz for the same charges.

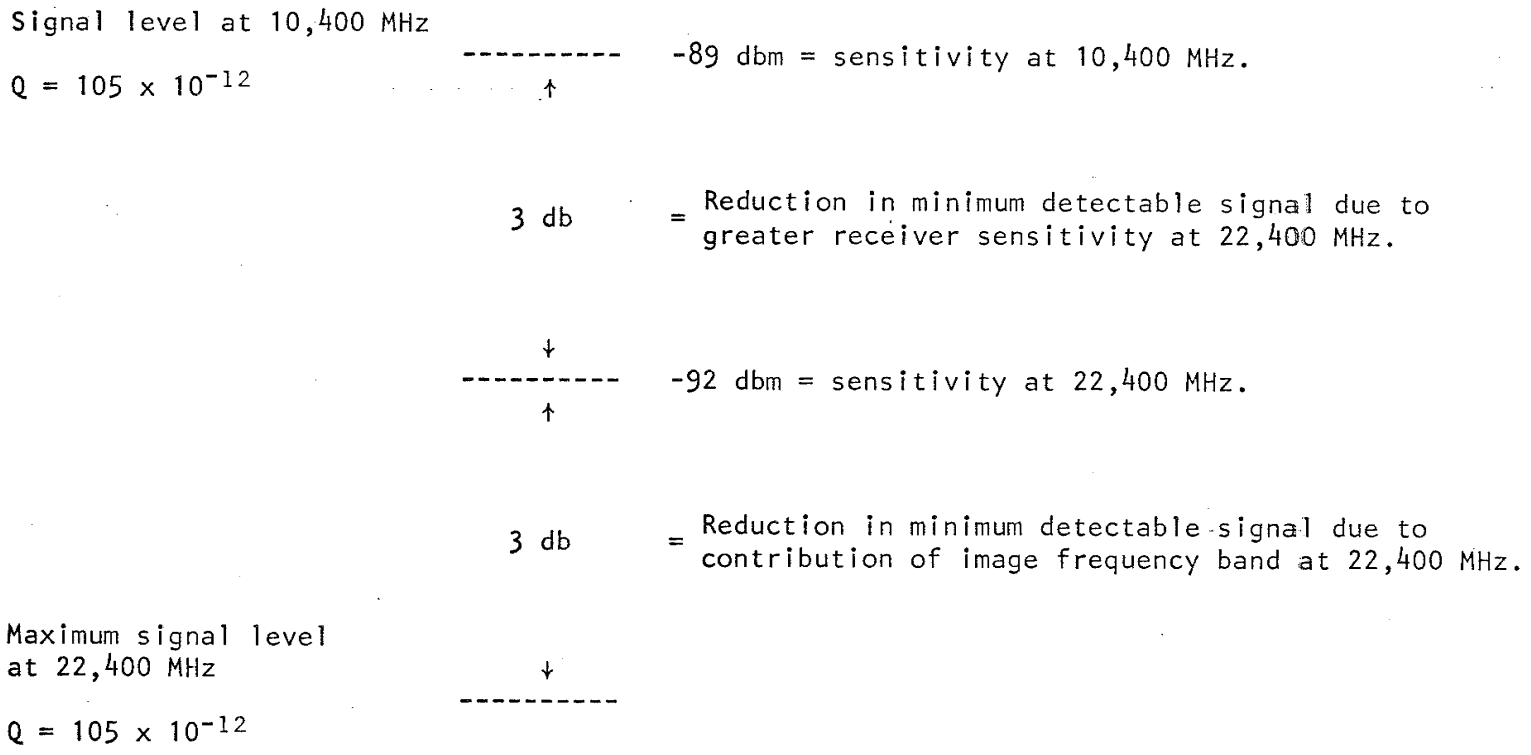

Figure 7. The estimation of intensity at 22,400 MHz.

The energy measurements were normalized by computing the energy radiated per unit solid angle in a direction perpendicular to the line of drop centers. For small solid angles the intensity was essentially uniform over the antenna aperture. Any small error introduced by assuming uniformity was common to all measurements since the solid angle subtended by the antennas was constant.

Let E_t = energy emitted/unit solid angle

and E = receiver input inergy.

Then $E = E_t\left(\frac{G\lambda^2}{4\pi R^2}\right)$

where $\frac{G\lambda^2}{4\pi R^2}$ is the solid angle.

In terms of the base energy intensity E_o,

$$\frac{E_t}{E_o} = \frac{E}{E_o}\ \frac{4\pi R^2}{G\lambda^2}$$

Taking logarithms and converting to decibels,

$$10 \log \frac{E_t}{E_o} = 10 \log \frac{E}{E_o} + 10 \{\log 4\pi + 2 \log R - \log G - 2 \log\lambda\}$$

Values of $10 \log E_t/E_o$, normalized according to this relation, are given in Tables I-IV in the following section.

Drop size was found by collecting a known number n of drops and computing the equivalent spherical diameter from the volume V of water collected.

$$d = \left(\frac{6V}{\pi n}\right)^{1/3}.$$

Even the most casual observation reveals that freely falling water drops are seldom spherical. Nevertheless, this is a convenient and generally accepted means of expressing size.

Charge per drop was measured in a correspondingly straightforward way by collecting drops at a known rate in an insulated brass cup (Figure 2) which was grounded through an electrometer. The indicated current (10^{-7} to 10^{-8} ampere in this experiment) gave the average charge per drop when divided by the number of drops per second.

The equipment just described had limitations which restricted the range of observations to that reported in the following section.

At best the energy emitted by the discharge between drops is small, and as the energy is reduced the signal pulses eventually become smaller than the noise pulses originating in the receiving system. The receiver noise level was reduced appreciably by using low noise preamplifiers at 7200 MHz and 9300 MHz, but these were not available at the higher frequencies. The significance of receiver noise level can be seen in Figure 9, where we see that the lowest detectable signal level at 7200 MHz was 19 db lower than the detectible signal level at 10,400 MHz.

The upper limit of microwave emission was imposed by the maximum charge which could be placed on the drops. The method of drop production depended on inducing instability in a water jet and, in consequence of this, the drops which formed underwent oscillation for a time after leaving the jet. The addition of large amounts of charge to these oscillating drops caused the drops to break up. This effect imposed an upper limit on drop charge.

Particularly severe limits on available drop size were imposed by the drop generator. Drops of certain discrete sizes (e.g., 0.8 and 1.05 millimeters) could be produced in monodisperse streams, but streams of other sizes were accompanied by accessory streams of smaller drops. When charged, these smaller drops usually were deflected electrostatically in precisely the manner required to drench the drop generator and disable the induction rings. This unfortunate characteristic of the drop generator is thought to be due to spurious mechanical vibrations which induced undesirable perturbations in the water jet.

At various times during the course of the microwave measurements the light emission was observed. This was done with a photomultiplier tube placed near the microwave antenna and a few centimeters from the discharge. Light pulses detected in this way were viewed on the dual-beam oscilloscope. The usual procedure was to view the microwave and light pulses at the same time.

The following section contains the experimental results and observations.

RESULTS

The principal result of this experiment was the observation and measurement of the energy emitted by the electric discharge between pairs of 1.05 millimeter diameter drops with equal and opposite charges in the range of 85×10^{-12} to 115×10^{-12} coulomb. Smaller drop pairs (0.8 millimeter diameter) with charges of up to 59.3×10^{-12} coulomb emitted no detectable microwave energy, although light emission was observed. In addition, the discharge of a 1.05 millimeter drop to a mass of water of approximately twice the drop volume and bearing relatively small charge was observed to produce light but no detectable microwave energy over the range of charge stated above.

Measurements of the microwave emission intensity E_t were made at four frequencies for various values of charge. These measurements are shown graphically in Figures 8 and 9 and tabulated in Tables I-IV.

Figure 8 is a logarithmic plot of the normalized intensity against frequency for increasing values of charge. This plot reveals the presence of a peak in the emission intensity, at about 10,000 MHz, which exhibits a regular increase in magnitude with charge.

Figure 9 illustrates the second major feature of the microwave emission, namely the strong dependence of intensity on charge. The curves shown are logarithmic plots of the normalized intensity against charge for different values of frequency. The linearity of the curves over at least a portion of their length indicates an exponential relation between intensity and charge. Evaluation of the exponent (the slope of the linear portion of the curve) from the values of charge and

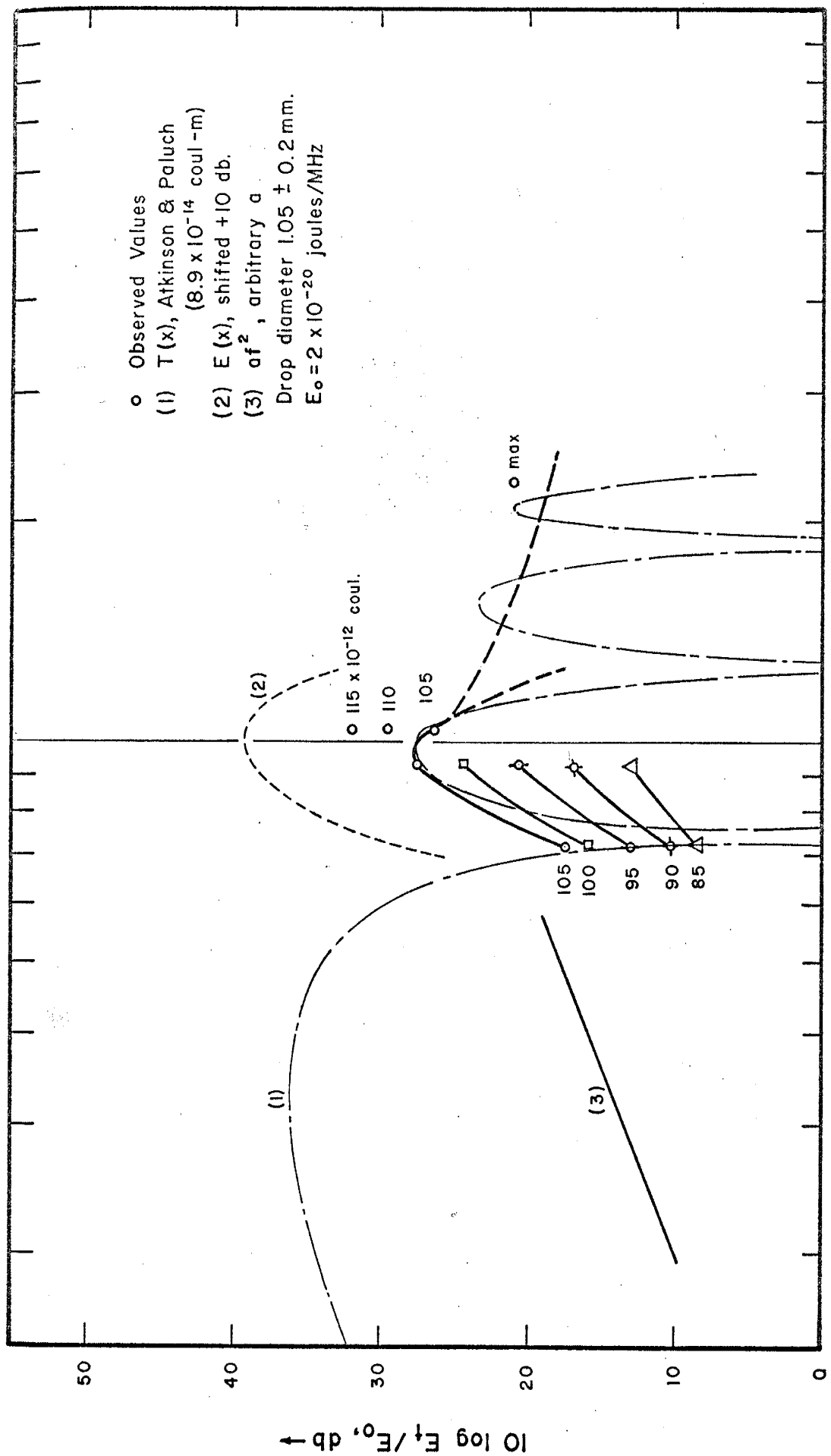

FIGURE 8. Microwave intensity; the variation with frequency as a function of charge

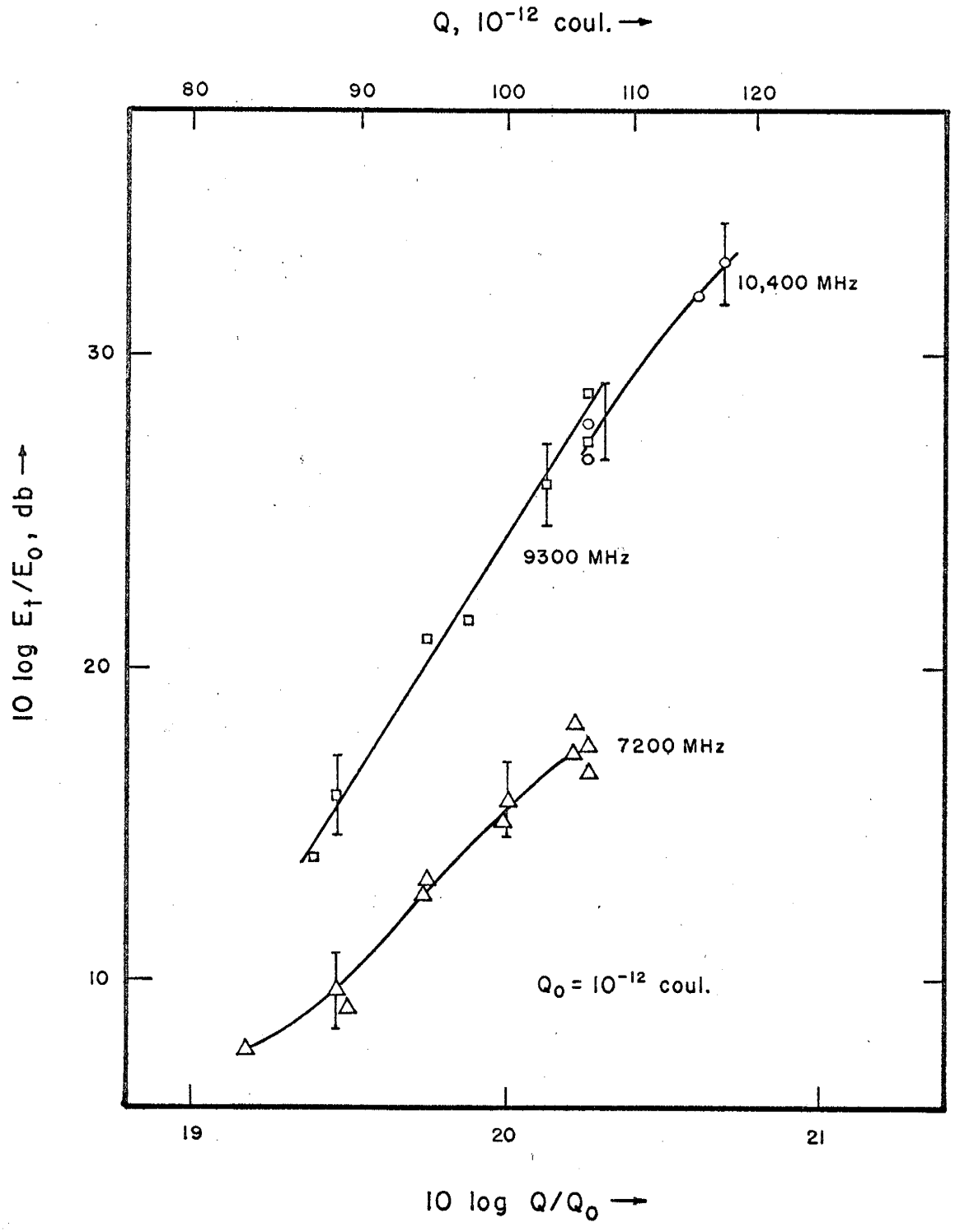

FIGURE 9. Microwave intensity; the variation with charge as a function of frequency

TABLE I: Measured Spark Emission Intensity

frequency = 7200 MHz wavelength = 4.16 centimeters

1967 Date	Drop Diameter millimeters		Charge 10^{-12} coulombs		10 log E_t/E_o db	Range centimeters
	-	+	-	+		
6 June	1.06	1.06	94.3	94.3	13.2	10
			88.6	88.6	9.1	
			82.6	82.6	7.8	
8 June	1.06	1.05	105	106	18.2	12.4
			100	100	15.8	
			94.1	94.1	12.8	
			88.4	88.4	9.7	
			88.4	88.4	9.7	
			94.1	94.1	12.8	
			97.7	102	15.1	
			106	106	16.7	
18 June			105	105	17.3	12.4
			106	106	17.5	

$E_o = 2 \times 10^{-20}$ joules/MHz.

Receiver: Polarad Model R with traveling wave tube preamplifier.

Antenna: Standard gain horn, 15.2 db gain at 7200 MHz.

Drop Composition: Socorro tap water.

TABLE II: Measured Spark Emission Intensity

frequency = 9300 MHz wavelength = 3.22 centimeters

1967 Date	Drop Diameter millimeters		Charge 10^{-12} coulombs		10 log E_t/E_o db	Range centimeters
	-	+	-	+		
31 May	0.8	0.8	59.3	58.2	< 10.0	10
3 June	1.05	1.05	106	106	27.4	10
			102	104	25.9	
4 June	1.03	1.03	94.3	94.3	20.9	10
			88.4	88.4	15.9	
			85.0	88.4	13.9	
	1.0	1.0	94.3	100	21.5	10
15 June	1.05	1.05	106	106	28.9	11
			106	106	27.9	

$E_o = 2 \times 10^{-20}$ joules/MHz.

Receiver: NMIMT radiometer receiver with tunnel diode amplifier and wave guide filter.

Antenna: Standard gain horn, 15.7 db gain at 9300 MHz.

Drop Composition: Socorro tap water.

TABLE III: Measured Spark Emission Intensity

frequency = 10,400 MHz wavelength = 2.89 centimeters

1967 Date	Drop Diameter millimeters		Charge 10^{-12} coulombs		10 log E_t/E_o db	Range centimeters
	-	+	-	+		
12 June	1.05	1.05	117	117	33.0	10
			113	117	32.0	
			105	106	26.7	
			106	106	27.8	

$E_o = 2 \times 10^{-20}$ joules/MHz.

Receiver: NMIMT radiometer receiver with filter.

Sensitivity: -89 dbm to 2 microsecond pulse.

Antenna: Standard gain horn, 16.5 db gain at 10,400 MHz.

Drop Composition: Socorro tap water.

TABLE IV: Measured Spark Emission Intensity

frequency = 22,400 MHz wavelength = 1.34 centimeters

1967 Date	Drop Diameter millimeters		Charge 10^{-12} coulombs		$10 \log E_t/E_o$ db	Range centimeters
	-	+	-	+		
28 June	1.05	1.05	109	109	detectable signal	3.7
			106	106	no detectable signal	3.7

$E_o = 2 \times 10^{-20}$ joules/MHz.

Receiver: NMIMT radiometer receiver.

Sensitivity: -92 dbm to 2 microsecond pulse.

Antenna: Standard gain horn, 14.6 db gain at 22,400 MHz.

Drop Composition: Socorro tap water.

intensity in Tables I-IV gives the following mean relations between intensity and charge:

$E_t = A \quad Q^{11}$ at 7200 MHz,

$E_t = A \quad Q^{15}$ at 9300 MHz,

$E_t = A \quad Q^{13}$ at 10,400 MHz, A constant.

Taking account of the probable maximum error in intensity (Error Analysis section) the limiting values of the exponent a (the slopes of the curves in Figure 9) can be computed from the value of charge and intensity in Tables I-IV.

For example, the maximum and minimum slopes at 9300 MHz are, from values in Table II,

$$a\begin{bmatrix}\max\\ \min\end{bmatrix} = \frac{(10 \log E_t/E_o)_1 - (10 \log E_t/E_o)_2 \pm 2 \times 1.1 \text{ db}}{(10 \log Q/Q_o)_1 - (10 \log Q/Q_o)_2 \pm 2 \times 0.03}$$

$$= \frac{25.9 - 15.9 \pm 2.2}{20.12 - 19.46 \pm 0.06}$$

$$= 20, 11$$

The maximum and minimum values of a found in this way are

$7 < a < 16$ at 7200 MHz.

$11 < a < 20$ at 9300 MHz.

$7 < a < 20$ at 10,400 MHz.

In cases where the charges on a pair of drops are not quite equal the average value is used.

The discharge between 0.8 millimeter diameter drops with charge of up to 59.3×10^{-12} coulomb produced light but no detectable microwave emission (Table II). At values of charge above 33.6×10^{-12} coulomb each collision resulted in light emission. For charges of 28.1×10^{-12} coulomb light pulses were produced by most of the collisions, but occasional misses occurred. At 22.4×10^{-12} coulomb sparking was very infrequent.

Under certain circumstances discharge occurred between a highly charged drop (1.05 millimeter diameter) and a larger mass of water bearing comparatively small charge. The mass of water was formed by the coalescence of the preceding drop pair and was in the form of a thin circular sheet. This sheet of water could be made to contact one of the incoming charged drops. When this occurred light was emitted but no microwave energy was detected. The drop did not coalesce with the sheet, but proceeded on to collision with its mate with reduced charge. The microwave emission intensity in this case showed some variation in magnitude, but was never observed to be greater than that resulting from the discharge between fully charged drops. The emission data plotted in Figures 9 and 10 pertain to those collisions in which this process did not occur.

Concurrent observation of microwave and light emission also revealed that, in general, the two quantities go together. That is, an increase in light intensity was accompanied by an increase in microwave intensity at all frequencies investigated.

The larger drops (1.05 millimeter) were produced at the rate of about 850 per second. Referring to Figure 3 we see that the drops move through a distance of about 3 drop diameters (3 millimeters) in the time of one cycle (1/850 second). Since the angle between drop streams was about 90°, the relative approach velocity was approximately

$$1.4 \times 3 \times 10^{-3} \times 850 = 4 \text{ meters/second.}$$

The smallest angle between streams was about 60°, giving a minimum relative velocity of 2.7 meters/second. The largest angle was about 90°, giving a range of relative velocity between 2.7 and 4 meters/second. These velocities were sufficient to cause coalescence of the drops whether charge was present or not but no variation in microwave emission with approach velocity was observed.

ERROR ANALYSIS

Intensity: The accuracy of this measurement depended principally on the antenna gain, range, uniformity of the impulse generator output, reference and signal attenuation, and null accuracy.

The antenna gains were specified by the manufacturers. As a check on the stated accuracy, the two low frequency horns were compared by use of a third horn and the Polarad receiver. The calculated gain ratio agreed with the measured ratio within 0.6 db.

Range was measured ±1 millimeter, the uncertainty being due to drop position. The expected error was largest at 22,400 MHz where the range was 3.7 centimeters. The accuracy here was ±2.7 per cent. At the other frequencies the limit was ±1 per cent.

The impulse generator output was specified uniform (+ 0.5 db) by the manufacturer. The limits were modified by subtracting 0.25 db from the measured values of 10 log E_t/E_o and expressing the uncertainty in the impulse generator output as ±0.25 db.

The waveguide fixtures, variable attenuators, and cables were calibrated against the Hewlett-Packard power meter, which was in turn calibrated against a d.c. standard. The accuracy of the power meter was found to be ±2 per cent (±0.1 db). The maximum calibration error was taken to be ±0.5 db to account for variations in waveguide flange connections, cable flexure, and the like.

From the oscilloscope display of the receiver impulse output the detectable change in level was found to be ±1 db. This was taken as the null error.

The accuracy of charge measurement was determined primarily by the electrometer, which was calibrated against the laboratory standard and found to agree within -0.9 to -0.4 per cent at scale values of 0.72 to 1 x full scale, respectively. On the assumption that the error varied linearly over the range of 0.72 to 1 x full scale, the measured values of charge were corrected by adding appropriate numbers in the range +0.9 to +0.4 per cent of the indicated value. The charge values given in Tables I-IV contain this correction. The remaining principal error was that associated with reading the scale. This was taken to be half a scale division or 0.5 per cent of full scale. The smallest value of Q was measured at 0.72 of full scale. The maximum error, 0.7%, occurred here.

The various sources of uncertainty in intensity are tabulated in the following table. The rms error was computed in the usual way by squaring the individual terms, summing and taking the square root after first converting the errors in db to fractional errors.

Probable Limits of Error in Intensity and Charge:

	7200 MHz	9300 MHz	10,400 MHz	22,400 MHz
Null error, db	±1.0	±1.0	±1.0	±1.0
Calibration error, db	±0.5	±0.5	±0.5	±0.5
Antenna error, db	±0.2	±0.3	±0.3	±0.2
Uncertainty in reference energy level, db	±0.25	±0.25	±0.25	±0.25
Range error, db	±0.05	±0.05	±0.05	±0.1
Rms intensity error, db	1.1	1.1	1.1	1.1
Charge measurement error, db	±0.03	±0.03	±0.03	±0.03

The probable contributions of the static and induction fields of the discharge can be shown to be negligible.

Drop Size: The diameter was found from volume and time measurements. Accuracy of the volume measurement was ±0.5 per cent. Time accuracy was ±1 second in 180 seconds, or 0.6 per cent. The rms error was estimated to be 0.8 per cent.

Frequency: The three lower frequencies were found with the Polarad Model R receiver, with stated accuracy of ±1 per cent of dial reading. Checks wherever possible against a microwave test set showed agreement. The 22,400 MHz frequency was ascertained by use of the Polarad Model DU-2 Spectrum Analyzer with accuracy of ±1 per cent of dial.

DISCUSSION AND CONCLUSIONS

General Discussion of Results: One interesting characteristic of the observed microwave emission is the strong dependence on charge (Figure 9). The capacitance of two spheres increases without bound as the spheres approach contact (Appendix B), so that the available electrostatic energy $Q^2/2C$ decreases rapidly at very close approach. Since the rate of increase of capacitance becomes very great (Figure 11) this fact alone may account for the observed variation of energy with charge since the distance between the drops at breakdown must increase with charge for constant breakdown potential difference between the drops. The drop separation, although much less than a drop diameter, is not known, nor is the shape of the drops, although they are probably not spherical.

The observation by Miller et al. (1965), that the optical emission is produced by a spark in air and the observation in the present work that an increase in available (electrostatic) energy is accompanied by an increase in both light and microwave emission suggest that the emission is connected in some way with the number of charged particles in the discharge. The spark discharge is a complex sequence of cataclysmic events beginning with the electron avalanche, and the ionization in the discharge channel depends strongly on the potential difference between the electrodes at the onset of discharge (Loeb and Meek, 1941). The discharge between water drops involves electric breakdown between moving fluid electrodes and is itself a complex phenomenon. Unfortunately, the existing knowledge of the discharge between water drops is not sufficiently definitive to support more than the simple suggestion that the

microwave emission intensity may depend on the number of charged particles in the discharge channel.

On the other hand, the large slope of the observed spectral intensity peak at 10,000 MHz (Figure 8) suggests the possibility of a resonance associated with the discharge.

The two drop system at the time of discharge may possess a resonant frequency due to the physical size of the drops and their relative positions.

Increases in discharge path lengths for increasing charges would tend to shift such a resonant frequency. However, due to the rapid decrease in electrostatic energy with decreasing drop separation the variation in path length is probably very small and the associated frequency shift might be undetectable in the present experiment. The investigation of microwave emission from discharges between drops of other than 1.05 millimeters diameter was not possible because of the limitations imposed by the drop generator.

The discharge plasma itself may possess a resonant frequency dependent on the electron or ion concentration. However, since the plasma dimensions are quite small compared with the wavelengths observed plasma resonance is probably not involved.

Based upon the microwave emission observations of Atkinson and Paluch (1965), the radiation field of discharging pairs of drops is sufficiently well represented by a dipole field. Let us represent the supposed oscillation by a dipole P suffering undamped harmonic motion for a finite number of cycles n.

$$p(t) = P \cos 2\pi f_o t, \quad -T \leq t \leq T \ ,$$

where $T = \frac{n}{2f_o}$

For convenience, we make the following substitutions:

Let $x_o = 2\pi f_o T$

and $x = 2\pi f T$.

Then $p(t) = P \cos \frac{x_o t}{T}$

and $\ddot{p}(t) = -P \frac{x_o^2}{T^2} \cos \frac{x_o t}{T}$.

If $g(x)$ is the Fourier transform of $\ddot{p}(t)$, then

$$2g^2(x) = \frac{p^2 x_o^4}{T^4} \{ \frac{1 - \cos 2x_o \cos 2x + \sin 2x_o \sin 2x}{(x_o + x)^2}$$

$$+ \frac{1 - \cos 2x_o \cos 2x - \sin 2x_o \sin 2x}{(x_o - x)^2}$$

$$+ \frac{2 (\cos 2x - \cos 2x_o)}{x_o^2 - x^2} \ \}$$

$$= \frac{p^2 x_o^4}{T^4} N(x) \ , \quad x \geq o \ .$$

$N(x)$ is simply an abbreviation for the bracketed sinusoidal terms. The function $g(x)$ is real since it is the transform of an even function. The function $g^2(x)$ is real and even, and it is defined over the entire

frequency domain. So for convenience it is multiplied by 2 as given and considered over positive frequencies only.

The energy per unit frequency may be written

$$E'(x) = \frac{2g^2(x)}{6\pi\varepsilon_o c^3}, \qquad x \geq o$$

$$= \frac{p^2 (x_o)^4 N(x)}{6\pi\varepsilon_o c^3 T^4} \times 10^6 \quad \frac{\text{joules}}{\text{MHz}} .$$

This expression represents the energy radiated by the oscillating dipole over an entire sphere surrounding it. The quantity of interest is the energy radiated per unit solid angle in a direction perpendicular to the dipole axis. Inserting the correction factor $3/8\pi$, we have

$$E(x) = \frac{p^2 (x_o)^4 N(x)}{6\pi\varepsilon_o c^3 T^4} \times 10^6 \; \frac{3}{8\pi}$$

$$= 1.05 \times 10^{-9} \; p^2 f_o^4 \; N(x) \qquad \frac{\text{joules}}{\text{MHz steradian}} .$$

The function $E(x)$ exhibits a maximum at $f = f_o$, the slopes of the peak increasing with n. The choice of $f_o = 10^{10}$ Hz and $n = 2.8$ results in the form shown in curve 2 of Figure 8. The computed total time duration, $2T$, is 2.8×10^{-10} seconds.

From the observed data the intensity at f_o is estimated to be about 30 db above E_o, or 2×10^{-17} joules/MHz steradian. Putting this value for $E(x)$ into the preceding equation, we may solve for the necessary dipole moment, P.

$$P = \left\{ \frac{2 \times 10^{-17}}{1.05 \times 10^{-9} f_o^4 N(x_o)} \right\}^{1/2}$$

$$= 1.2 \times 10^{-15} \text{ coulomb - meters.}$$

For drops bearing charge of $\pm 50 \times 10^{-12}$ coulombs, Atkinson and Paluch (1966) report that direct measurement of the dipole moment change during discharge gave a value of 10^{-14} coulomb - meters. The dipole moment change during discharge of $\pm 105 \times 10^{-12}$ coulomb drops is probably greater than 10^{-14} coulomb - meters and hence greater than the value of P calculated above. That is, the available dipole moment is more than sufficient to produce the observed emission by simple dipole oscillation. The function E(x) cannot alone account for the observed emission since it would produce no net charge transfer, but the example does serve to illustrate the possibility of a resonance superimposed on the decay of the dipole moment. E(x), as plotted in curve 2 of Figure 8, has been arbitrarily shifted in the vertical direction to avoid clutter.

The minimum energy spectrum deduced by Atkinson and Paluch is plotted as curve 1 of Figure 8 for comparison with observed results.

$$S(x) = \frac{9 \sin^2\theta (\Delta p)^2}{16\pi^2 c^3 \varepsilon_o R^2 \tau^2} \frac{1 + x^2 - 2x \sin 2x - \cos 2x + x^2 \cos 2x}{x^4}$$

$$\frac{\text{joules}}{\text{meter}^2 \text{ Hz}},$$

$$x = 2\pi f\tau \geq 0.$$

In this form the function is not quite appropriate dimensionally for comparison with the observed intensity. The energy intercepted by an

antenna of effective aperture A is S(x)A, but A/R^2 is just the solid angle subtended by the antenna aperture. So we define

$$T(x) = S(x)A \times \frac{R^2}{A} = \text{joules/Hz steradian.}$$

$$T(x) = \frac{9 \sin^2\theta (\Delta p)^2 10^6}{16\pi^2 c^3 \varepsilon_0 \tau^2} \cdot \frac{1 + x^2 - 2x \sin 2x - \cos 2x + x^2 \cos 2x}{x^4}$$

$$\frac{\text{joules}}{\text{MHz steradian}} .$$

T(x) is the function plotted in Figure 8. The value of τ was selected to place the second peak at 9,800 MHz by the relation

$$\tau = 15/16\ f_{max} = 9.6 \times 10^{-11} \text{ seconds.}$$

This represents a total discharge duration of 2τ or 1.9×10^{-10} seconds. The value of Δp was set arbitrarily at 8.9×10^{-14} coulomb - meters. Since $\theta = \frac{\pi}{2} \pm 15^o$ over the antenna aperture, $\sin^2\theta \approx 1$.

The function T(x) shows some similarity to the observed spectral intensity for the particular values chosen for τ and Δp. However, the zero of T(x) at about 7500 MHz does not agree with the observation that a signal was emitted continuously over the frequency range of 7200 MHz for several values of charge about 105×10^{-12} coulomb.

Applications to Radiometry: In connection with radiometric observations of the atmosphere (of either Earth or Venus), an estimate of the relative magnitudes of thermal (black body) radiation and drop discharge emission is of interest.

Dicke et al. (1946) show that an antenna in equilibrium with its surroundings delivers power to a matched receiver with level determined by the temperature and absorption along the path defined by the antenna beam. At temperatures and frequencies such that $hf << kT$, where h is Planck's constant, the relation between power and temperature, for complete absorption, is given as

$$P = k\,T\,\Delta f.$$

This notion has been extended by Lhermitte (1965) to relate the observed temperature to absorption by a cloud of water drops. If the apparent temperature T_e is much smaller than the average temperature T of the cloud and the cloud drop diameters are less than .04 times the wavelength, then

$$\frac{T_e}{T} = \frac{1}{4.34} \int_0^\infty \alpha(z)\, dz$$

where $\alpha(z)$ = the absorption coefficient

$$= 4.34 \times 10^3 \frac{6\pi}{\lambda} \frac{M}{\rho} \text{Im}\ (-K) \qquad \text{db/kilometer}$$

and λ = wavelength, meters

M = liquid water concentration, kilograms/meter^3

ρ = density of water, kilograms/meter^3

$K = \frac{m^2 - 1}{m^2 + 2}$, m = complex refractive index

Im $(-K)$ = 0.0335 at 9300 MHz and 0°C (Gunn and East, 1954).

The following simple model is employed to estimate T_e. Assume the radiometer antenna beam is filled with a uniform cloud of millimeter diameter drops for a distance of 1 kilometer.

Let $M = 0.01$ kilograms/meter^3

$\lambda = 3.2 \times 10^{-2}$ meters

$\rho = 10^3$ kilograms/meter^3

$\bar{T} = 273^{\circ}K.$

Then

$$\frac{T_e}{T} = \frac{1}{4.34} \alpha(z) \Delta z$$

$$= 0.21$$

$$T_e = 57^{\circ}K.$$

If the frequency dependence is ignored, the power originating from drop discharges can be expressed in terms of an apparent temperature at a selected frequency.

$$P = k T_a \Delta f.$$

In the model above, assume that discharges between drop pairs occur at the rate of n discharges per second per cubic meter with dipoles oriented to produce maximum signal. If the antenna (assumed circular) is uniformly illuminated (Silver, 1949),

then $x = \frac{\lambda}{D}$, the half-power beamwidth,

and $A = \frac{\pi D^2}{4}$, the antenna absorption cross section,

where D = physical diameter.

$$P = n\left(\frac{\text{collisions}}{\text{meter}^3\ \text{sec}}\right) E_t \left(\frac{\text{joules}}{\text{MHz steradian}}\right)$$

$$\times \frac{\pi D^2}{4R^2}\ (\text{steradians}) \times \frac{\lambda^2\ R^2\ \pi\Delta z}{D^2 4}\ (\text{meter}^3) \times \Delta f$$

$$= \frac{nE_t\ \pi^2\lambda^2\Delta z}{16} \times 10^{-6}\ \Delta f = k\ Ta\ \Delta f\ \text{watts}$$

and

$$T_a = \frac{nE_t\ \pi^2\lambda^2\Delta z \times 10^{-6}}{16k} .$$

The value of E_t is taken from Figure 9 as 27 db above E_o or 10^{-17} joules/MHz steradian at 9300 MHz (λ = 3.2 centimeters), corresponding to charges of $\pm 105 \times 10^{-12}$ coulomb per drop pair, and we have

$$T_a = 0.45\ n .$$

Denoting the number of drops per cubic meter by N,

$$N = \frac{6M}{\pi d^3 \rho} = 2 \times 10^4\ \frac{\text{drops}}{\text{meter}^3}$$

If $T_a = T_e = 57^o$,

then $\frac{n}{N} = \frac{28.5}{0.45} \times 10^{-4} = 0.006\ \frac{\text{collisions}}{\text{second}}$, or

6 collisions/second per thousand drops.

This estimate assumes the existence of a mechanism tending to align the discharges. Random orientation of the discharges in time and space is estimated to reduce the detected energy due to the sin θ and cos ϕ dependence by a factor of $(4/\pi^2)^2$, obtained by averaging sin θ and cos ϕ over half cycles of θ and ϕ. The charges involved are about twice

those reported from thunderstorm measurements (Gunn, 1957). Because of the strong dependence on charge, a reduction of charge by a factor of two would reduce the emission to an undetectable level.

Limits on the Relative Magnitudes of Discharge Emission and Thermal Emission from a Cloud of Water Drops: There are certain natural limits on the amount of charge that a water drop of a given size may hold.

The Rayleigh criterion predicts the maximum free surface charge Q as a function of radius r, where α is the surface tension.

$$Q \leq \{ 4\pi\varepsilon_o \alpha 16\pi r^3 \}^{1/2} \text{ coulomb.}$$

For greater values of Q the electrostatic stress exceeds the surface tension force and the drop disrupts. Doyle et al. (1964) have obtained experimental results in agreement with this expression.

The result of a study by Taylor (1964) concerning the disruption of uncharged water drops in an external electric field states that the maximum uniform field F_o in which a drop can exist is given by

$$F_o \leq 1.6 \{\alpha/r\}^{1/2} \text{ cgs - esu}$$

or

$$F_o \leq 4800 \{\alpha/r\}^{1/2} \text{ volts/meter}$$

where α = surface tension of water, dynes/centimeter

and r = drop radius, meters.

If the water drop is assumed to remain spherical up to this limit, the induced polarization charge may be calculated readily by integrating

the surface charge density over one hemisphere. Doing this, we get

$$Q = 3\pi r^2 \varepsilon_o F_o .$$

Inserting the expression for F_o we get the maximum induced charge as a function of drop radius.

$$Q \leq 3.5 \times 10^{-6} r^{3/2} \text{ coulomb}$$

where α = 75 dynes/centimeter and r is in meters.

This is the maximum induced polarization charge a spherical water drop is capable of holding at 273°K according to the Taylor criterion.

For comparison we restate the two criteria just discussed.

$$Q = 21 \times 10^{-6} r^{3/2} \text{ coulomb; (free charge).}$$

$$Q = 3.5 \times 10^{-6} r^{3/2} \text{ coulomb; (polarization charge).}$$

where r is the drop radius in meters. We see that, for a given radius, the maximum free charge exceeds the maximum induced charge by a factor of 6.

The application of the Taylor criterion to a spherical drop is not quite accurate, since at fields near breakdown the drop becomes elongated in the direction of the field. However, the electric stress tending to disrupt the drop surface depends on the surface charge density, which is maximum at the tip of the distorted drop and which decreases with distance from the tip. So it seems clear that, in any event, the total maximum induced charge is less than the maximum free charge predicted by the Rayleigh criterion.

Since the energy of discharge between drops increases with charge, the Rayleigh criterion puts an upper bound on the energy as a function of the drop radius. We can now compare the maximum discharge emission with thermal (black body) radiation from a cloud of drops as a function of drop radius and collision rate.

The effective equilibrium radiometer antenna temperature T_e due to a cloud of water drops at thermodynamic temperature $\bar{T}$ filling the antenna beam is

$$T_e = \bar{T} \frac{6\pi\ M\Delta z\ \mathrm{Im}(-K)}{\lambda\ \rho}\ {}^{o}K \quad .$$

The apparent antenna temperature due to spark discharge between drops, as derived previously, is

$$T_a = \frac{n\ E_t\ \pi^2\ \lambda^2\ \Delta z\ 10^{-6}}{16\ k}\ {}^{o}K.$$

And the number of drops per cubic meter N is simply

$$N = \frac{3M}{4\pi r^3 \rho} \text{ in consistent units.}$$

The experimental observations (Table II) give the following relation between intensity E_t and charge Q

$$E_t = 8.1 \times 10^{132}\ Q^{15}\ \frac{\text{joules}}{\text{MHz steradian}} \text{ at 9300 MHz,}$$

$$\text{for } 88 \times 10^{-12} < Q < 103 \times 10^{-12} \text{ coulomb.}$$

Substituting the expression for maximum free charge,

$$Q \leq 2.1 \times 10^{-5}\ r^{3/2} \text{ coulomb,}$$

and assuming E_t is not explicitly a strong function of r, we get

$$E_t = 5.4 \times 10^{62}\ r^{22.5}\ .$$

Putting the value of E_t into the expression for T_a and taking the ratio of T_a to T_e,

$$\frac{T_a}{T_e} = 1.1 \times 10^{71}\ \frac{nr^{19.5}}{N}\ .$$

The ratio (n/N) is simply the number of collisions per drop per second, the normalized collision rate.

If we let $n/N = 1$ and $T_a/T_e = 1$, then

$$\frac{T_a}{T_e} = 1.1 \times 10^{71}\ r^{19.5} = 1$$

and $r = 0.23$ millimeters.

If we let $n/N = 10^{-6}$ and $T_a/T_e = 1$, then

$$\frac{T_a}{T_e} = 1.1 \times 10^{65}\ r^{19.5} = 1$$

and $r = 0.47$ millimeters.

The condition of $n/N = 1$ is the very rapid collision rate of 1 collision per drop per second and it probably does not occur in an atmospheric cloud. So we conclude that for cloud drops smaller than 0.23 millimeters radius the spark emission is probably negligible.

The collision rate $n/N = 10^{-6}$ collisions/drop per second is less stringent and the emission may be detectable. In this case distinction

can be made on the basis of spectral form. At ordinary temperatures the thermal emission increases as the square of the frequency at microwave frequencies, while the spark emission increases much more rapidly. Figure 8 contains an arbitrary f^2 curve for comparison with the observed intensity. Simultaneous intensity measurement at two frequencies should serve to separate the thermal emission from the spark emission.

This conclusion should be qualified by noting that the present work deals with drops of a single size. Investigation of emission from drops of different sizes is needed. If a frequency shift of the spectral peak due to drop size dependence exists, it might tend to obscure the distinction between spark and thermal emission.

The Anomalous Microwave Brightness of Venus: On the assumption that the discharge process is operative on Venus and assuming that the experimental results are valid there, we can estimate the contribution to the apparent microwave brightness temperature $\bar{T}$ (Figure 10). The thermodynamic temperature T_o is not frequency dependent and could be represented by a horizontal line lying below the measured values shown in Figure 10. At 22,400 MHz the excess of apparent temperature T_a, above T_o, is assumed to be due to the spark discharge. From Figure 8 the minimum ratio of intensities due to drop discharge at 10,400 MHz and 22,400 MHz is 6 db, or a factor of 4 so that the excess temperature at 10,400 MHz is 4 T_a. We can now write two equations in the variables T_o and T_a.

$$T_o + 4T_a = 580^{\circ}K \text{ at } 10{,}400 \text{ MHz } (\lambda = 2.89 \text{ centimeters}).$$

$$T_o + T_a = 400^{\circ}K \text{ at } 22{,}400 \text{ MHz } (\lambda = 1.34 \text{ centimeters}).$$

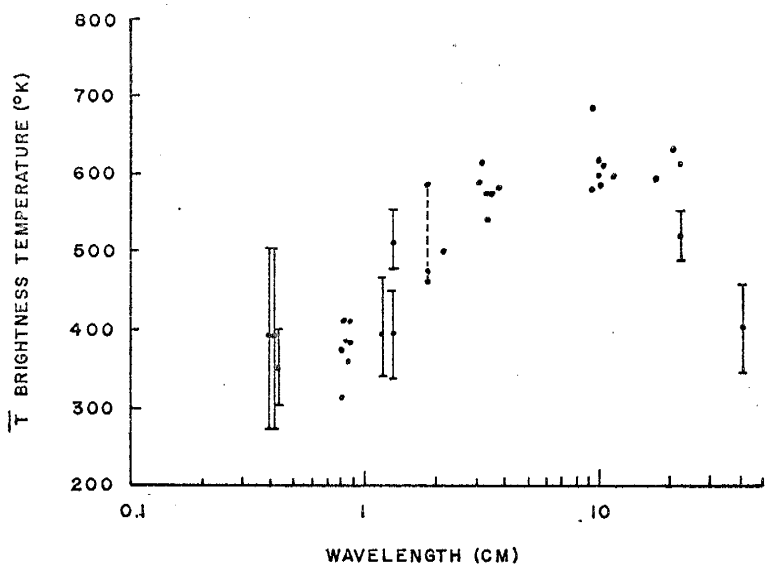

FIGURE 10. The Microwave Brightness of Venus
(Taken from Plummer and Strong, 1965)

Solution of this set of equations gives

$$T_a = 60^{\circ}K \quad \text{and} \quad T_o = 340^{\circ}K.$$

On the basis of the present drop discharge observations, this value of T_a is a maximum.

Since the maximum microwave brightness temperature of Venus occurs in the region of $\lambda = 10$ centimeters, the corresponding values of spark emission intensity must be found before conclusions can be drawn. The elementary consideration here assumes no factors other than drop discharge emission are operative in determining the frequency dependence of the Venusian microwave brightness. Since little is known of the conditions existing in the Venusian atmosphere, the computation above should be regarded as an exercise, not as an analysis of conditions existing there.

The drop size-collision rate relation for fully charged drops as derived previously, is

$$\frac{T_a}{T_e} = 1.1 \times 10^{71} \frac{nr^{19.5}}{N}$$

If the Venusian atmosphere is dense to microwaves, we may set

$$T_e = T_o = 340^{\circ}K.$$

If $T_a = 60^{\circ}K$, then

$$\frac{T_a}{T_e} = \frac{60}{340} = 1.1 \times 10^{71} \frac{nr^{19.5}}{N}$$

For illustration let us set r = 0.47 millimeters.

Then $\frac{n}{N} = 1.6 \times 10^{-72} r^{-19.5}$

$= 1.8 \times 10^{-7}$ collisions/drop per second.

If the average apparent temperatures T_a and T_o over the visible hemisphere of Venus are 60^o and 340^o respectively, then the necessary collision rate between fully charged drops of 0.47 millimeter radius is 1.8×10^{-7} collisions per drop per second.

Conclusions: The measurements of microwave emission intensity resulting from the collision of and discharge between 1.05 millimeter diameter drops bearing equal and opposite charges have been reported and discussed in the preceding pages. These data show that a spectral intensity maximum exists at the frequency of approximately 10,000 MHz and that the magnitude of the intensity increases rapidly with increasing charge over the range of frequency considered (7200 MHz to 10,400 MHz).

The state of knowledge of the drop discharge is not sufficiently complete to permit postulation of a mechanism for generating the emission, but the strong charge dependence of the emission does suggest a possible connection with the formation of charged particles in the discharge channel. The intensity function T(x) derived analytically by Atkinson and Paluch does not quite describe the observed emission. The reader may recall that T(x) is the spectral intensity function which yields the minimum total energy radiated by an electric dipole undergoing change Δp in time 2τ. We may conclude, then, that drop discharge mechanism simply does not radiate the minimum possible total energy.

On the assumption that the observed intensity-charge relationship is not an explicit function of the drop diameter and that the observed relation holds for small charges the maximum contribution from the discharge microwave emission can be compared to the thermal (black body emission) from a cloud of water drops in a planetary atmosphere. This computation has been done in the preceding pages, and the results indicate that discharge emission is equal to thermal emission for a cloud of drops of radius 0.23 millimeters if one collision per drop occurs each second and if the drops bear maximum electric charge. A similar cloud of 0.47 millimeter (radius) drops emits equal discharge emission if the collision rate is one collision per million drops per second. We conclude from this analysis that discharge from the smaller drops ($r < 0.23$ millimeters) is probably insignificant in our atmosphere. Under the assumption stated above, the maximum spark emission increases strongly with drop radius since the maximum charge increases with radius so that for larger drops emission of this type may be detectable.

Conclusions regarding the apparent microwave brightness of Venus should await discharge measurements at wavelengths around 10 centimeters. Magnitude calculations based on present evidence were given in the preceding sub-section and they indicate no great restrictions on drop sizes and collision rates required to account for the anomalous brightness at 1.34 and 3.2 centimeters.

RECOMMENDATIONS

While the study presented in the preceding pages cannot be called comprehensive, in the sense of investigating all the variables, the observations do clearly point out the importance of charge in determining the magnitude of the microwave emission. The suggestion that the rapid increase in emission may be associated simply with an increase in the number of charged particles in the discharge plasma is consistent with the observation that the light intensity and microwave intensity increase with the available energy. Simultaneous measurement of light and microwave intensities now might be useful. If the light emission is found to increase strongly with charge, this would indicate that the light and microwave emission are produced by the same process, which may be related in some way to the ionization of the discharge plasma.

Light intensity measurement was not attempted in this experiment because the need was not apparent at the outset. However, the measurement should not present great difficulty. It could be made in some detail with a simple photomultiplier tube, a standard light source for calibration, and a set of filters appropriate to the spectral emission lines found by Miller et al. (1965).

The nature of the physical process associated with the spectral peak at 10,000 MHz is another question raised but unresolved by the present study. The need for further examination of the emission spectrum as a function of drop size is clearly indicated. That a resonant frequency is associated with drop size has been shown by Stratton (1941), who treated analytically the case of spheres of infinite conductivity. The

lowest order oscillation (longest wavelength) is given by the relation $\lambda = 7.3r$ for the case of infinite conductivity.

The observed peak for water drops exists at a wavelength given by the relation

$$\lambda = 60r.$$

This wavelength appears rather long to be associated with the resonance as treated by Stratton, even when the effect of a finite conductivity is considered. However, that treatment concerns single isolated spheres. The pair of water drops may represent coupled harmonic oscillators with frequencies of oscillation $f_o + \Delta f$ and $f_o - \Delta f$, where f_o is the frequency of either oscillator alone. The combined effects of strong coupling and frequency decrease due to the dielectric properties of water might account for the observed position of the spectral peak. However, consideration of a resonance based on drop size should await experimental observation of such an effect.

As mentioned in the preceding section, a certain practical significance may be attached to the possible drop size dependence of the spectral peak in connection with radiometric observation of atmospheric clouds. With an adequate drop generator, the investigation of the emission from drop pairs of various sizes is a straightforward procedure.

The question of the occurrence of a natural oscillation of the discharge plasma might be clarified by a systematic investigation of the emission over a greater range of charge and at a greater number of frequencies about 10,000 MHz. A number of complete spectral curves like the one at 105×10^{-12} coulomb of Figure 8 might reveal a systematic shift in the peak frequency which could be attributed to changes in

charge density in the discharge. This set of measurements can be made with the aid of an adequate drop generator capable of producing more highly charged drops.

The microwave brightness temperature of Venus is maximum at the wavelength of about 10 centimeters (Figure 10). Observation of drop discharge emission at this wavelength is desirable to test any explanation of the Venus temperature on the basis of discharge between water drops.

In conclusion, the set of observations reported here indicates two major features of the microwave emission from colliding charged water drops. These observations represent an advance in the state of knowledge of the phenomenon, but they are not comprehensive. Further observations over wider ranges of the variables (frequency, charge, drop size) are required before the phenomenon can be understood.

DEFINITIONS AND ABBREVIATIONS

Some of the following terms have more than one meaning. The proper interpretation of these symbols is clear in the context in which they are used. RMKS units are used throughout unless otherwise specified.

c	the speed of light, 3×10^8 meters/second
C	capacitance
d	drop diameter
db	decibel, 10 log (power or energy ratio)
dbm	decibel with respect to a power level of one milliwatt
D	antenna aperture width or diameter
E	the general term for energy or energy intensity
E_o	the standard intensity, 2×10^{-20} joules/MHz
E_t	emission intensity, energy per unit frequency per unit solid angle, polarized with electric vector in the direction of the spark discharge and propagated in a direction perpendicular to the line of discharge, joules/MHz steradian
f	frequency
G	gain
h	Planck's constant, 6.62×10^{-34} joule-seconds
Hz	cycles per second
k	Boltzmann's constant, 1.38×10^{-23} joules/^oK
kMHz	kilomegacycles (10^9 cycles) per second
^oK	degrees Kelvin
log	logarithm to the base 10
MHz	megacycles (10^6 cycles) per second
M	liquid water concentration, gram/meter^3

$p(t)$	dipole moment (time dependent)
$\dot{p}(t)$	first time derivative of $p(t)$
$\ddot{p}(t)$	second time derivative of $p(t)$
Δp	increment of dipole moment
P	dipole moment (constant); power
q	electric charge
Q	electric charge
r	drop radius
R	range
t	time
T	time duration; temperature
W	electrostatic energy
α	surface tension
$\alpha(z)$	absorption coefficient, db/unit length
ε_o	the permittivity of free space, $\frac{10^{-9}}{36\pi}$ $\frac{\text{farads}}{\text{meter}}$
λ	wavelength
ρ	density
τ	time duration
θ	angle between the line of spark discharge and the direction of observation
ϕ	angle between the line of discharge and the polarization plane of the antenna

APPENDIX

Appendix A: The Magnitude of E_o.

The magnitude of E_o, the arbitrarily selected standard output of the Polarad Impulse Generator is deduced from the calibration procedure stated by the manufacturer.

The output of the impulse generator is a pulse of very short duration 2T, which is sampled by a receiver with bandwidth $\Delta f = 1$ MHz, and the output is indicated on a peak-reading volt meter. The impulse level is defined in terms of a sine wave receiver input. That is, an impulse level producing the same receiver output as a sine wave of amplitude 1 microvolt rms (1.41 microvolts peak) is termed 1 microvolt/MHz.

The peak value of the receiver impulse output may be found by taking the Fourier transform of the impulse, selecting a band of frequencies, $\Delta f = 1$ MHz, within the region of uniform spectral amplitude, and reconstructing the time pulse.

Define the impulse function $V_o(t)$ as follows:

Let $V_o(t) = A \quad , \qquad -T \leq t \leq T.$

Then the Fourier transform $g(f)$ of $V_o(t)$ is

$$g(f) = 2 \int_o^T A \cos 2\pi ft \, dt$$

since $V_o(t)$ is an even function.

$$g(f) = 2AT \left(\frac{\sin 2\pi fT}{2\pi fT} \right) .$$

In the uniform region of the spectrum $2\pi fT$ is very nearly zero, so

$$g(f) \doteq 2AT.$$

The receiver output $V_1(t)$ is reconstructed by use of the inverse Fourier transform taken over frequencies defined by the bandwidth Δf. The choice of the low frequency limit is immaterial and is chosen to be zero for convenience.

$$V_1(t) = 2 \int_0^{\Delta f} 2AT \cos 2\pi ft \, df$$

since $g(f)$ is even.

$$V_1(t) = 4AT\Delta f \left(\frac{\sin 2\pi\Delta ft}{2\pi\Delta ft} \right).$$

The maximum of $V_1(t)$ occurs at $t = 0$.

$$V_1(0) = 4AT\Delta f.$$

$$\frac{V_1(0)}{\Delta f} = 4AT = 2\, g(f).$$

The spectral amplitude function $g(f)$ is now defined in terms of the receiver peak voltage output and bandwidth. The peak voltage $V_1(0)$ corresponding to the peak voltage of a 1 microvolt rms sine wave is

$$V_1(0) = 1.4 \text{ microvolts}.$$

So $$2\, g(f) = \frac{1.4 \text{ microvolts}}{1 \text{ MHz}};$$

$$g(f) = 0.7 \text{ microvolt/MHz}.$$

This is the spectral amplitude function specified uniform over the range of frequency 1 MHz to 10,000 MHz by the manufacturer. The energy contained in the band Δf and dissipated in a 50 ohm load is

$$E_o \Delta f = \frac{1}{50} \int_{-\Delta f}^{\Delta f} g^2(f)\, df$$

$$= \frac{2}{50} \int_{o}^{\Delta f} g^2(f)\, df \,,$$

$$= \frac{2}{50}\, g^2(f)\Delta f, \text{ since } g^2(f) \text{ is uniform.}$$

$E_o = 2 \times 10^{-20}$ joules/MHz per impulse.

Appendix B: The Capacitance and Dipole Moment to Two Conducting Spheres of Equal Size and Charge.

The problem of capacitance is solved in Page and Adams, Principles of Electricity (p. 87) by the method of images. Details are given in that reference and will not be repeated here. If the radius of the spheres is r and the distance between centers b, the capacitance is given by

$$C = 2\pi \varepsilon_o r S$$

where ε_o = permittivity of free space (air)

$$S = 1 + m + m^2 + m^3 + 2m^4 + 3m^5 + \ldots$$

$$m = \frac{r}{b} .$$

The series S can be shown to converge for $m < \frac{1}{2}$.
If the spheres are in contact, $m = \frac{1}{2}$ and the series S diverges. This is consistent with the fact that at contact the two spheres are at the same potential. In this case the potential difference between the spheres is independent of the charge, i.e. the capacitance is infinitely large.

The value of C is used in estimating the energy available for radiation by the discharge from the relation

$$W = \frac{1}{2} \frac{Q^2}{C} .$$

The capacitance is found by use of an infinite series of images, q_1, q_2, . . . $-q_1$, $-q_2$, . . . separated by distances ℓ_1, ℓ_2, . . .

This representation may also be used for computing the dipole moment.

$$P = q_1 \ell_1 + q_2 \ell_2 + \ldots$$

The components of this series, as derived from Page and Adams, are as follows:

Charge, q_i	Moment arm, ℓ_i
q_1	b
mq_1	$b - 2mr$
$\frac{m^2 q_1}{1-m^2}$	$b - \frac{2mr}{1-m^2}$

etc.

Evaluating the series through m^4 terms,

$$P = q_1 S' b$$

$$S' = 1 + m + m^2 - m^3 - 0 + \ldots$$

The total charge, $Q = q_1 S$, where S is defined previously.

$$P = Q b \frac{S'}{S}$$

When $m = \frac{1}{2}$, $b = d = 2r$, and $P = 0$, consistent with the fact that the net charge, at contact between drops, is reduced to zero.

The behavior of C, P, and W is diagrammed in Figure 11.

For a somewhat different treatment of the two sphere (or sphere to infinite plane) problem the reader may refer to pages 1298 to 1300 of Methods of Theoretical Physics by Morse and Feshbach.

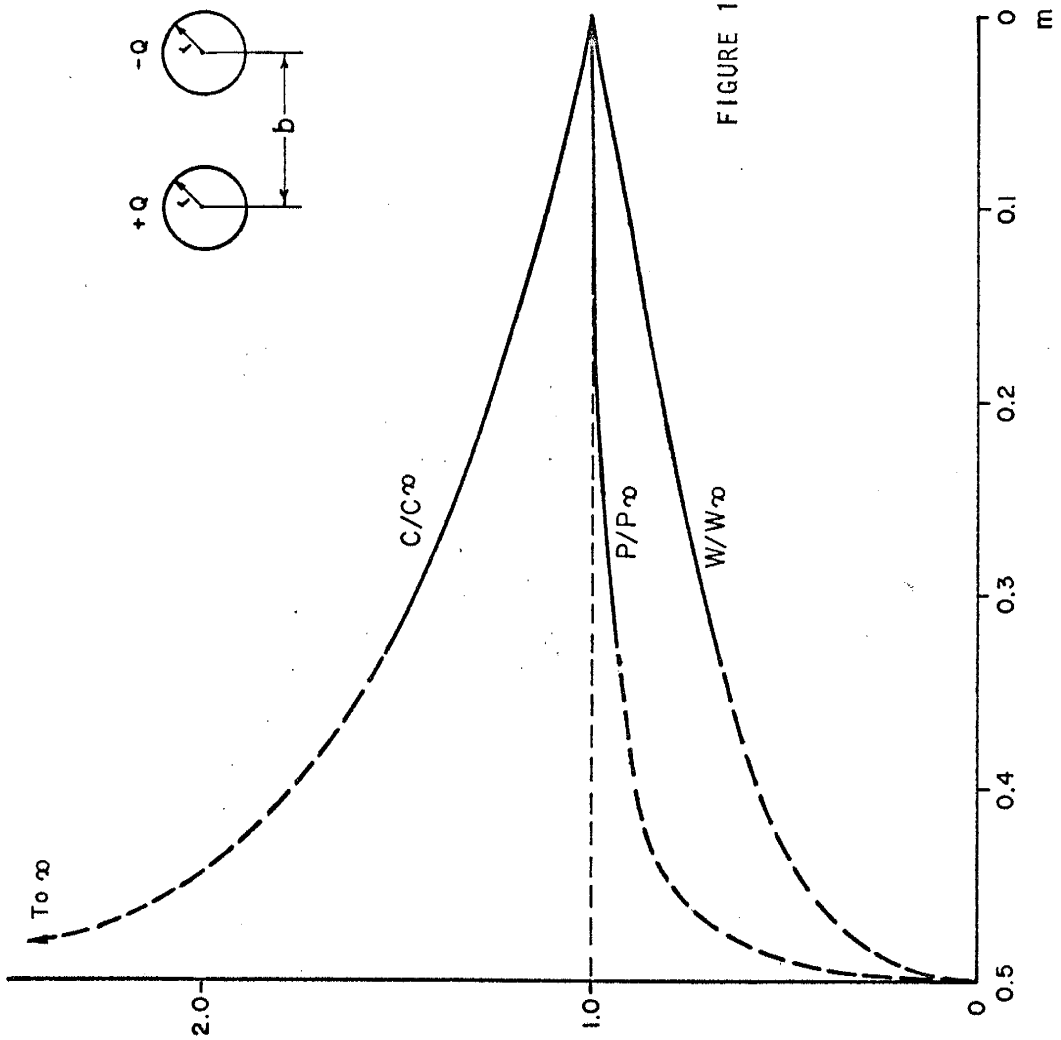

FIGURE 11. The capacitance, dipole moment, and electrostatic energy of two equal spheres bearing equal and opposite electric charges

Appendix C: Equipment.

Universal Eput and Timer, Beckman Model 7360

High Voltage Power Supply, Fluke Model 405B 0-3000V

High Voltage Power Supply, Beta Electric 0-5000V

Voltage Regulator, Stabiline Type 1E5101R, 60 cycle, single phase

Pulse Generator, Lavoie Laboratories, LA-593

Power Supply/Amplifier, Harrison 6823A (3)

Electrometer, Keithley 610A with shielded test lead

Strobotac, General Radio Type 1531A

Lock-In Amplifier, Princeton Applied Research, Model JB-4

Oscilloscope, Tektronix Type 555 Dual Beam, Type CA Plug-in unit

Impulse Generator, Polarad Model 1C120A

Microwave Power Meter, Hewlett-Packard, 431B with 478A coaxial thermistor mount

Photomultiplier, RCA C-7222 with power supply

7200 MHz

Microwave Receiver, Polarad Model R with RX-T FR tuning unit

Standard Gain Horn, DeMornay-Bonardi DBJ-520 15 db at 7000 MHz

Traveling Wave Tube Amplifier, Watkins-Johnson WJ-271

9300 MHz

NMIMT radiometer receiver

Tunnel Diode Amplifier, International Microwave Corp., Model AWR 9250-15

Power Supply, Harrison Model 865-B, 0-40V

Standard Gain Horn, Narda Model 640

Wave Guide Filter, Frequency Standards, Model 50B19700

Amplifier, Hewlett-Packard, Model 450A

Radar Test Set, General Communications, Model TS-642/u.

10,400 MHz

NMIMT Radiometer Receiver

Standard Gain Horn, Narda Model 640

Waveguide Filter, Frequency Standards, Model 50B19700

Amplifier, Hewlett-Packard, Model 450A

Signal Generator, Polarad SG-57/URM-36

Converter, 60 cycle to 400 cycle, Industrial Test Equipment Co., Model 250

22,400 MHz

NMIMT Radiometer Receiver

IF Preamplifier, RHG Model FT 6010 BAL

Standard Gain Horn, DeMornay-Bonardi, DBE-520 15 db @ 23,500 MHz

Amplifier, Hewlett-Packard, Model 450A

Spectrum Analyzer, Polarad Model DU-2 with STU-4W Plug-in unit

Klystron Power Supply, PRD Type 815

Klystron Power Supply, Hewlett-Packard Type 716B

Power Supply, Fluke Model 407

BIBLIOGRAPHY

BIBLIOGRAPHY

Atkinson, W. R., and C. E. Abbott, Epoch Sensitivity of Superheterodyne Microwave Receivers to Electromagnetic Pulses Produced by Electrical Discharge between Water Drops, To be published in Journal of Geophysical Research, Vol. 72, No. 20, October 15, 1967.

Atkinson, W. R., and Ilga Paluch, Electromagnetic Emission from Pairs of Water Drops Exchanging Charge, Journal of Geophysical Research, Vol. 71, No. 16, August 15, 1966, p. 3811.

Atkinson, W. R., and J. D. Sartor, Laboratory Studies of Charge Transfer between Water Drops with Application to Radio Meteorology, Twelfth Conference on Radar Meteorology, Norman, Oklahoma, October 17-20, 1966, p. 164.

Dicke, R. H., R. Beringer, R. L. Kyhl, and A. B. Vane, Atmospheric Absorption Measurements with a Microwave Radiometer, Physical Review, Vol. 70, Nos. 5 and 6, September 1 and 15, 1946, p. 340.

Doyle, A., D. R. Moffett, and B. Vonnegut, Behavior of Evaporating Electrically Charged Droplets, Journal Colloid Science 19, 1964, pp. 136-143.

Drake, F. D., Improbability of Non-Thermal Radio Emission from Venus Water Clouds, The Astrophysical Journal, Vol. 149, August 1967, pp. 459-461.

English, W. N., Positive and Negative Point-to-Plane Corona in Air, Physical Review, Vol. 74, No. 2, July 15, 1948, p. 170.

English, W. N., Corona from a Water Drop, Physical Review, Vol. 74, No. 2, July 15, 1948, p. 179.

Gibson, J. E., Some Observations of Microwave Radiation from Clouds, NRL Memorandum Report 693, March 27, 1957.

Gibson, J. E., Atmospheric Attenuation at K-Band Radio Wavelengths, NRL Report 4966, August 8, 1957.

Gunn, K. L. S., and T. W. R. East, The Microwave Properties of Precipitation Particles, Quarterly Journal Royal Meteorological Society, 80, 1954, p. 522.

Gunn, R., The Electrification of Precipitation and Thunderstorms, Proceedings I R E, October 1957, p. 1331.

Hogg, D. C., Effective Antenna Temperatures Due to Oxygen and Water Vapor in the Atmosphere, Journal of Applied Physics, Vol. 30, No. 9, September 1959, p. 1417.

Hogg, D. C., and R. A. Semplak, Effect of Rain and Water Vapor on Sky Noise at Centimeter Wavelengths, Bell Telephone System Monograph 3974, 1961.

Lhermitte, R. M., Indirect Probing of Cloud and Precipitation by Microwave Radiometer, Preprint 40.2-1-65, Instrument Society of America, October 4-7, 1965.

Loeb, L. B., and R. A. Wijsman, The Theoretical Criterion for Streamer Advances in an Electric Field, Journal of Applied Physics, Vol. 19, August 1948, p. 797.

Loeb, L. B., Recent Developments in Analysis of the Mechanisms of Positive and Negative Coronas in Air, Journal of Applied Physics, Vol. 19, October 1948, p. 882.

Miller, A. H., C. E. Shelden, and W. R. Atkinson, Spectral Study of the Luminosity Produced during Coalescence of Oppositely Charged Falling Water Drops, Physics of Fluids, Vol. 8, No. 11, November 1965, p. 1921.

Plummer, W. T., and J. Strong, Conditions on the Planet Venus, Astronautica Acta, Vol. 11, 1965, No. 6, p. 375.

Plummer, W. T., and J. Strong, An Answer to F. D. Drake, The Astrophysical Journal, Vol. 149, August 1967., p. 463-4.

Sartor, J. D., Radio Observation of the Electromagnetic Emission from Warm Clouds, Science, Vol. 143, p. 948.

Sartor, J. D., Radio Emission from Clouds, Journal of Geophysical Research, Vol. 68, No. 18, September 15, 1963, p. 5169.

Taylor, G. I., Disintegration of Water Drops in an Electric Field, Proceedings Royal Society (London) A280, 1964, p. 383.

Tolbert, C. W., and A. W. Straiton, A Consideration of Microwave Radiation Associated with Particles in the Atmosphere of Venus, Journal of Geophysical Research, Vol. 67, No. 5, May 1962, p. 1741.

Zeleny, J., On the Conditions of Instability of Electrified Drops, with Applications to the Electrical Discharge from Liquid Points, Physical Review, N. S., Vol. 2, 1914, p. 69.

BIBLIOGRAPHY: METHODS AND TECHNIQUES

Atkinson, W. R., and A. H. Miller, Versatile Techniques for the Production of Uniform Drops at a Constant Rate and Ejection Velocity, Review of Scientific Instruments, Vol. 36, No. 6, 1965, p. 846.

Gunn, R., The Synchrodropper-A Versatile Tool, American Journal of Physics, Vol. 33, No. 10, October 1965, p. 824.

Mason, B. J., O. W. Jayaratne, and J. D. Woods, An Improved Vibrating Capillary Device for Producing Uniform Water Droplets of 15 to 500 μm Radius, Journal Scientific Instruments, Vol. 40, 1963, p. 247.

GENERAL REFERENCES

Bracewell, R., The Fourier Transform and its Applications, McGraw-Hill Book Co., New York, 1965.

Brown, Sanborn C., Basic Data of Plasma Physics, The Technology Press of the Massachusetts Institute of Technology and John Wiley & Sons, Inc., New York.

Loeb and Meek, The Mechanism of the Electric Spark, Stanford University Press, Stanford University, California, 1941.

Loeb, L. B., Experimental Contributions to the Knowledge of Charge Generation, Chapter VII of Thunderstorm Electricity, edited by H. R. Byers, University of Chicago Press, 1953.

Loeb, L. B., Basic Processes of Gaseous Electronics, University of California Press, Berkeley and Los Angeles, 1955.

Morse, P. M., and H. Feshbach, Methods of Theoretical Physics, McGraw-Hill Book Co., Inc., 1953.

Page, L., Introduction to Theoretical Physics, D. Van Nostrand Co., Inc., Princeton, N. J., 1952.

Page, L., and N. I. Adams, Principles of Electricity, D. Van Nostrand Co., Inc., Princeton, N. J., 1958.

Silver, S., Microwave Antenna Theory and Design, Massachusetts Institute of Technology Radiation Laboratory Series, Vol. 12, McGraw-Hill Book Company, 1949.

Stix, T. H., The Theory of Plasma Waves, McGraw-Hill Book Company, 1962.

Stratton, J. A., Electromagnetic Theory, McGraw-Hill Book Company, 1941.

Terman, F. E., and J. M. Pettit, Electronic Measurements, McGraw-Hill Book Co., Inc., New York, 1952.

This thesis is accepted on behalf of the faculty of the Institute by the following committee:

Stuart A. Colgate

Ralph M. McGehee

A. J. Petschek

C. B. Moore

Marx Brook

Date: Feb 20, 1968